Meteorologische Zeitschrift, PrePub DOI 10.1127/metz/2018/0905

A windthrow model for urban trees with application to storm "Xavier"

Günter Gross*

Institut für Meteorologie und Klimatologie, Universität Hannover, Germany

(Manuscript received January 21, 2018; in revised form May 17, 2018; accepted June 11, 2018)

Abstract

A three-dimensional meteorological micro-scale model was combined with a forestry windthrow tool to study the risk of urban trees under stormy conditions. The numerical results for an isolated individual tree are compared to general findings from forestry and pulling experiments in the field. It was found that the model is suitable to capture the critical wind speed in the right order of magnitude which causes strong hazards to trees. The new tool was applied to a limited real city environment during storm "Xavier", where significant and extensive tree damage have been observed. A comparison of the numerical results with the observations demonstrates a very reasonable agreement not only for the onset of windthrow but also for the right areal distribution during different phases of the storm.

Keywords: Micro-scale simulation, windthrow model, urban trees, "Xavier"

1 Introduction

Trees are indispensable and integral parts of the urban environment because of the multitude of advantages. Caused by modifications in the surface energy budget, temperatures in residential areas may occasionally be more than 10 K warmer than the nearby countryside (Kuttler, 2011). Trees reduce this heat island effect by lowering the air temperature through shade and an increased evapotranspiration. This results also in lowering heat stress levels and a significant improvement of outdoor thermal comfort for city residents (Lee et al., 2013). In a future climate, where we expect a temperature increase of 3–4 K, blue and green design elements are, in addition to a conversion of rural to urban areas and the essential reduction of air pollutant emissions, very effective and helpful measures to improve the urban climate (Gross, 2017; Shashua-Bar and Hoffman, 2004). Urban trees as an individual tree, an avenue or a park are known to have a wide range of benefits to plan and develop resilient and liveable cities (Salmond et al., 2016).

Besides the powerful advantages, trees may constitute also a danger to the residents. Depending on the species and the history of environmental stress during their lifespan like soil compaction, drainage problems, droughts and air pollution (Roloff, 2016), many trees can grow to large objects. With increasing tree height the wind forces acting upon stem and branches can be large, and as a last consequence major damage to parts or even stem breaking or uprooting of the entire tree may result during strong wind conditions. The resistance to such an uprooting increases with an effective root-soil plate anchorage. However, urban trees are more vulnerable because the anchorage is reduced by a limited root volume and modifications in root architecture, and wind forces are enhanced by specific air flow features in streets and around individual buildings. During high wind speed situations there is a potential safety risk posed to the public and infrastructure from falling branches and trees as happened in the very recent past. In 2014 high wind speeds triggered by the storm "Ela" damaged and uprooted more than 20,000 urban trees in the city of Düsseldorf (Germany). For a rather similar situation in 2017 during the passage of depression "Xavier" severe damage on several thousands of urban trees have been observed in many cities in the northern part of Germany.

Uprooting, stem breakage and other failures of trees by wind loads lead to significant costs for communities, extensive damage to urban infrastructure and danger to people. In order to enhance current knowledge and to understand the multitude of interactions between trees, wind and the environment, many experimental studies have been carried out in the field (e.g. Milne, 1991; Cermak et al., 2015) and in wind tunnels (e.g. Ruck and Schmitt, 1986; Wood, 1995) to identify the causes of tree failure.

In addition, models of different complexity are available to assess and forecast air flow and wind effects on individual trees (e.g. Gross, 1993; Kormas et al., 2016) and larger forest stands (Gardiner et al., 2008). Also in forestry it is of great importance to estimate possible damage and economic losses due to storms. Two mechanistic wind damage risk models are widely used for calculating the danger of windthrow for specific synoptic situations. The key component of the models HWIND (Peltola and Kellomäki, 1993) and GALES (Gardiner et al., 2000) is the calculation of a critical wind

*Corresponding author: : Günter Gross, Institut für Meteorologie und Klimatologie, Universität Hannover, Herrenhäuser Str. 2, 30419 Hannover, Germany, e-mail: gross@muk.uni-hannover.de

speed in excess of which severe storm damage of forests can no longer be prevented. In GALES, wind is calculated 10 m above the displacement height of a larger homogeneous coniferous forest, and model parameterizations are adjusted to typical situations in Scotland. In the HWIND model, the necessary wind information is calculated 10 m above ground downwind of the forest edge, and verification has been demonstrated for typical forests in Finland. Although both models are extremely helpful tools for practical applications, shortcomings are identified for other tree species and for complex stands and landscapes (Gardiner et al., 2008).

The distribution of meteorological variables within a city environment is significantly determined by existing trees. This has been demonstrated by urban applications of various building and stand resolved micro-scale models (Gross, 2012; Salim et al., 2015). In Bruse (2016) the wind risk of urban trees is addressed as well as longer term effects like vulnerabilities with respect to pests or water stress.

In the paper presented here, the basic findings from forestry mechanistic models are included in a micro-scale meteorological model. This new analysis tool can be used for urban tree protection by identifying wind endangered areas within a building environment.

2 The model system

Tree damage at a given location results from unfavourable or extreme conditions in wind, vegetation growth and soil properties. Windthrow results when wind-induced turning moments exceed root anchorage or stem strength and the entire tree is uprooted or the tree trunk fails at the weakest point. Further to the more extreme local climate conditions, trees in an urban environment are especially vulnerable because of the limited space for root growth and building-induced additional wind loads. In order to characterize the physical processes involved in tree uprooting and stem breakage, the three main factors air flow, tree characteristics and soil anchorage are combined in a numerical model. Such models are valuable tools to study the importance of individual factors, providing additional information about observed damaging events and optimizing tree management scenarios.

2.1 The tree model

The mechanistic model of Peltola and Kellomäki (1993) and Peltola et al. (1999) is adopted here as a guideline to estimate windthrow and stem breakage of individual trees. Although this model was developed for a single Scots pine at a stand edge it is used here in the absence of any more reasonable approach. The wind-induced force on a tree at height z above ground is calculated in this study using an aerodynamic drag equation

$$F_u(z) = 0.5 c_d \rho U(z)^2 b(z) \tag{2.1}$$

with empirical drag coefficient c_d, air density ρ [kg m^{-3}], mean wind speed U [m s^{-1}] and leaf area density b [m^2 m^{-3}]. For increasing wind speed the tree streamlines but wind-induced force is not growing as strong as Eq. (2.1) calculates. This effect is considered by a modification of c_d in line with Mayhead (1973) and Wood (1995):

$$c_d = 0.6 \exp(-0.0009779 U^2). \tag{2.2}$$

When the wind force F_u deflects the tree away from the vertical axis, an additional gravitational force is acting:

$$F_g(z) = M(z) g. \tag{2.3}$$

M [kg] is the green mass of the stem and crown at a certain height, and g [m s^{-2}] is the gravitational constant. The resulting turning moment T [N m] acting on the tree is calculated by

$$T(z) = \{F_u(z) z + F_g(z) x(z)\}\ gust. \tag{2.4}$$

z [m] is the height above the base of the tree, and x [m] is horizontal displacement from the vertical which is estimated by (Peltola and Kellomäki, 1993):

$$x(z) = \frac{F_u}{6\,MEL\,I} a^2 h_{\text{tree}} \left(3 - \frac{a}{h_{\text{tree}}} - 3\frac{l(z)}{h_{\text{tree}}}\right) \qquad z \geq a$$
$$x(z) = \frac{F_u}{6\,MEL\,I} \left(a^2 \left[2 - 3\frac{l(z)-d}{a} + \frac{(l(z)-d)^3}{a^3}\right]\right) \qquad z < a \tag{2.5}$$

In this equation, MEL [Pa] is the modulus of elasticity, $I = \pi DBH^4/64$ [m^4] is the area moment of inertia with stem diameter at breast height DBH [m], a [m] is the distance from ground level to crown centre, h_{tree} [m] is the tree height, $d = h_{\text{tree}} - a$ [m] and l [m] is the distance from the top. Extreme loads are considered by a gust factor $gust$ in Eq. (2.4) which is estimated by experimental findings.

The total turning moment at the base of the stem is calculated by summing up the contributions at different heights according to Eq. (2.4) and compared against thresholds for uprooting UP [N m] which represents the anchorage of the root-soil plate with characteristics mass m [kg] and mean depth h_{soil} [m]:

$$UP = \frac{g m h_{\text{soil}}}{A_{\text{soil}}}. \tag{2.6}$$

A_{soil} [%] is a parameter characterizing the ground anchorage (Coutts, 1986).

According to Peltola et al. (1999) it is assumed that a stem breaks if the maximum turning moment exceeds a threshold of

$$ST = \frac{\pi}{32} MOR\, DBH^3 \tag{2.7}$$

with the modulus of rapture MOR.

Although many shapes of trees can be reproduced in the model, only hollowed ellipsoidal shapes, representing a deciduous tree, are adopted in this study. The main

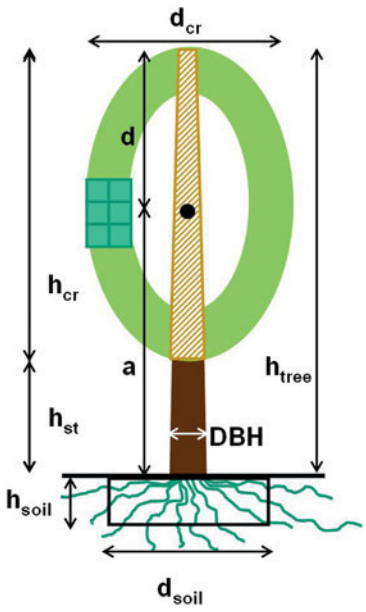

Figure 1: Schematic presentation of the tree model.

Table 1: Tree model parameters.

leaf area density [$m^2\,m^{-3}$]	1.0
stem density [$kg\,m^{-3}$]	850
taper	1:100
modulus of elasticity MEL [MPa]	7,000
modulus of rupture MOR [MPa]	30
depth of root-soil plate [m]	$h_{soil} = 0.9\,h_{tree}/20$
diameter of root-soil plate [m]	$d_{soil} = 1.35\,h_{tree}/20$
Contribution of root-soil plate weight to total anchorage [%]	30
soil density [$kg\,m^{-3}$]	1,500

tree parameters are shown in Fig. 1. In the crown with diameter d_{cr} and height h_{cr}, leaves are concentrated in the outer two grid volumes. The stem with a prescribed diameter at breast height *DBH* tapers from below to tree height h_{tree}, and for the root-soil plate, responsible for the anchorage, depth h_{soil} and diameter d_{soil} must be specified. Because of a lack of local tree information, plausible magnitudes of the parameter, which are within the range of observations, are adopted here to run the analysis tool. Except where noticed otherwise, tree characteristics necessary for the tree model as listed in Table 1 are used here (adopted and derived from Peltola and Kellomäki, 1993 and Peltola et al., 1999).

For typical and persistent wind conditions trees have developed an optimized structure to resist dynamical loads. During strong wind conditions this load will be much greater, as caused by occasional and sporadic wind gusts. At least in a crude approximation this effect can be considered by an empirical gust factor (Gardiner et al., 2008). The attempt to describe the complex interaction between turbulent wind and a single tree by a simple term results in a wide range of estimated gust factors. However, the range is not too large, and typical values are in the order of 1.5 to 2.5 (Mayer, 1985; Mayer and Schindler, 2002; Peltola et al., 1999; Jäger, 2014). In this study, a gust factor of $gust = 2.0$ is used.

2.2 The wind model

It appears from the above presentation that tree failure depends strongly on local wind force. To calculate wind distribution in a highly complex urban environment with buildings and trees, a micro-scale numerical model is used and combined with the tree model described above.

Mean wind and turbulence are calculated with the model ASMUS, which is based on the Navier-Stokes equations, the continuity equation and the first law of thermodynamics. The eddy exchange coefficient, introduced by Reynolds averaging and flux-gradient parameterization, is determined via the turbulence kinetic energy E by an additional prognostic equation. A detailed model description is given in Gross (2014). The tree canopy is considered as a porous structure with a three-dimensional distribution of leaf area density b. The effects of a tree canopy on the meteorological variables are parameterized following the pioneering work of Raupach and Shaw (1982) with an additional drag term. Mean wind components u_i are reduced according to

$$\frac{\partial u_i}{\partial t} = \ldots - c_d b u_i U \tag{2.8}$$

and turbulence is enhanced

$$\frac{\partial E}{\partial t} = \ldots c_d b U^3. \tag{2.9}$$

The boundary conditions for the mean wind at the ground and at the building surfaces are zero, and turbulence kinetic energy is proportional to the local friction velocity squared. The friction velocity is calculated assuming a logarithmic wind profile between the surface and the closest grid value in the atmosphere. At the upper boundary an undisturbed situation is assumed with given values for wind and turbulence kinetic energy, while at the lateral boundaries no-flux conditions for all variables are used.

The model equations are solved on a numerically staggered grid where all scalar quantities are arranged in the centre of the grid volume, while velocity components are defined at the corresponding side walls. The pressure disturbance is calculated by solving a three-dimensional discrete Poisson equation directly by Gaussian elimination in the vertical and fast Fourier transforms in the horizontal directions. Depending on the numerical study, a fine grid resolution of 0.5–2 m is used for all directions.

3 Results

The model system described above was used to study the effects of high wind conditions on individual idealized trees. First, a study with a single tree in a plain was performed to test the interactions against knowledge and findings from forestry. The application of the model for a realistic storm scenario in an urban environment will be discussed afterwards.

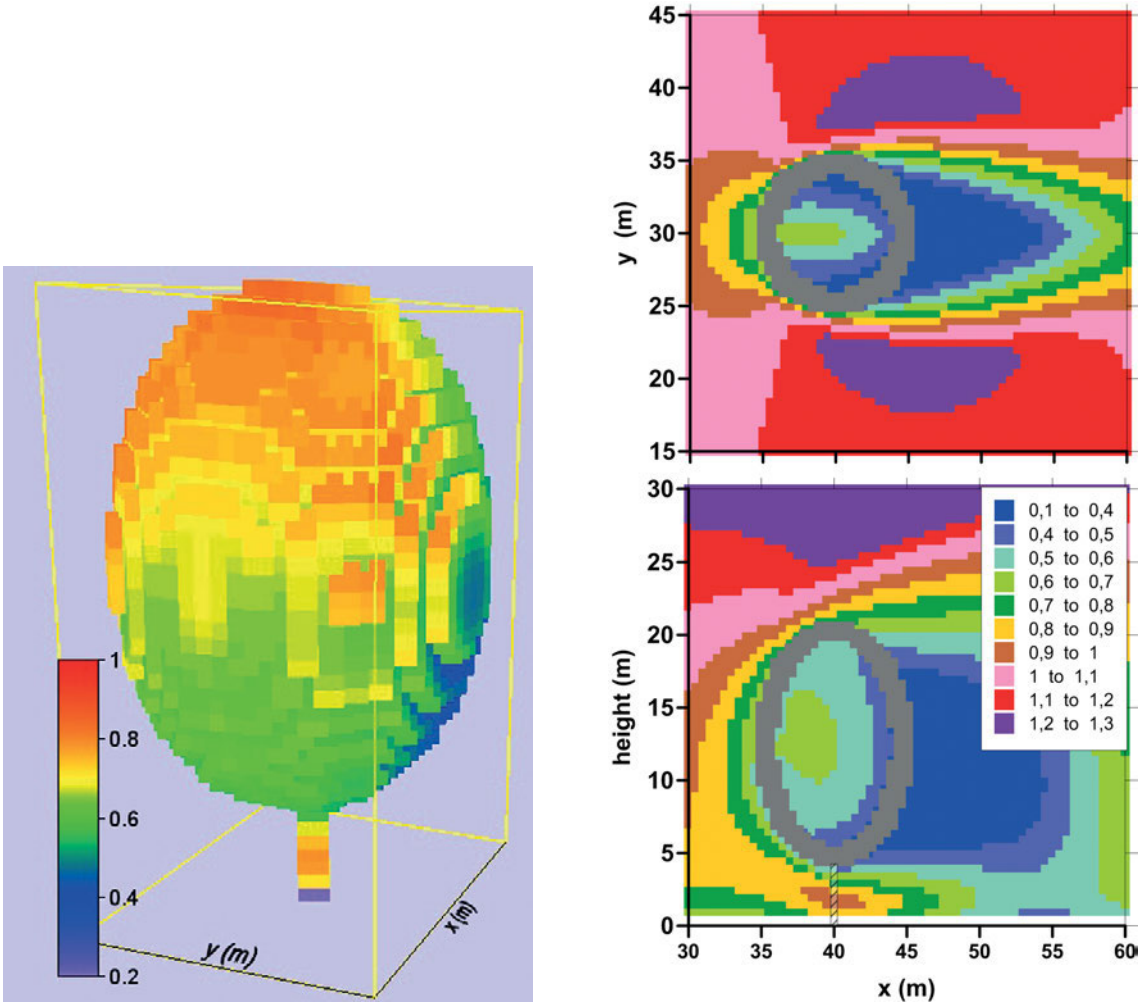

Figure 2: Mean wind speed normalized with the undisturbed 10 m value. Left: three dimensional distribution above the tree surface. Right above: horizontal cross section at a height of 12 m (middle of the crown) Right below: vertical cross section along the centre. Grey areas indicate leaf area.

3.1 Numerical experiment with a single tree

The air flow around and through individual trees has been studied in wind tunnels (e.g. Ruck and Schmitt, 1986; Gromke and Ruck, 2008) and with numerical models (e.g. Gross, 1993; Mochida et al., 2008). Based on these experiments a number of characteristic features are known, like higher winds near the top and along the sides of the tree, a wake region behind and a strong underflow in the stem region. These typical features of the air flow will be compared to the simulated results presented below. A 20 m high model tree with a 4 m stem and a ball-shaped crown with $d_{cr} = 10$ m and $h_{cr} = 16$ m was adopted here. Leaves are arranged in the outer two grid cells with constant leaf area density of $b = 1\,m^2\,m^{-3}$. The grid resolution in all directions is 0.5 m. For a neutral stratified atmosphere a logarithmic wind profile with surface roughness length of 0.01 m and a superimposed mean wind along the x-direction with $U = 10\,m\,s^{-1}$ at 10 m is prescribed.

In Fig. 2 the oncoming wind component, normalized with the undisturbed value at 10 m height, for small subsections of the total simulation region is presented in a horizontal cross-section through the centre of the crown and a vertical cross-section along the middle of the tree. From the vertical cross-section it is evident that the oncoming wind is forced to avoid the obstacle by an over- and underflow. High wind speeds are simulated near the top of the tree on the windward side and a secondary maximum in the trunk space. The air flow is strongly reduced in front of the tree but nevertheless enters the crown due to the streamlining of the tree elements.

The dominant feature behind the obstacle is a wake region with low wind speed. The specific structure of this wake depends strongly on the strength of the superimposed wind and the permeability of the tree with recirculation zone being smaller, extended, or even detached compared e.g. to solid bodies. The air flow is forced not only to go over the obstacle but also around by a lateral movement causing a wind speed maximum on both sides of the tree. This feature together with the lateral extension of the wake is shown in the horizontal cross-section in Fig. 2.

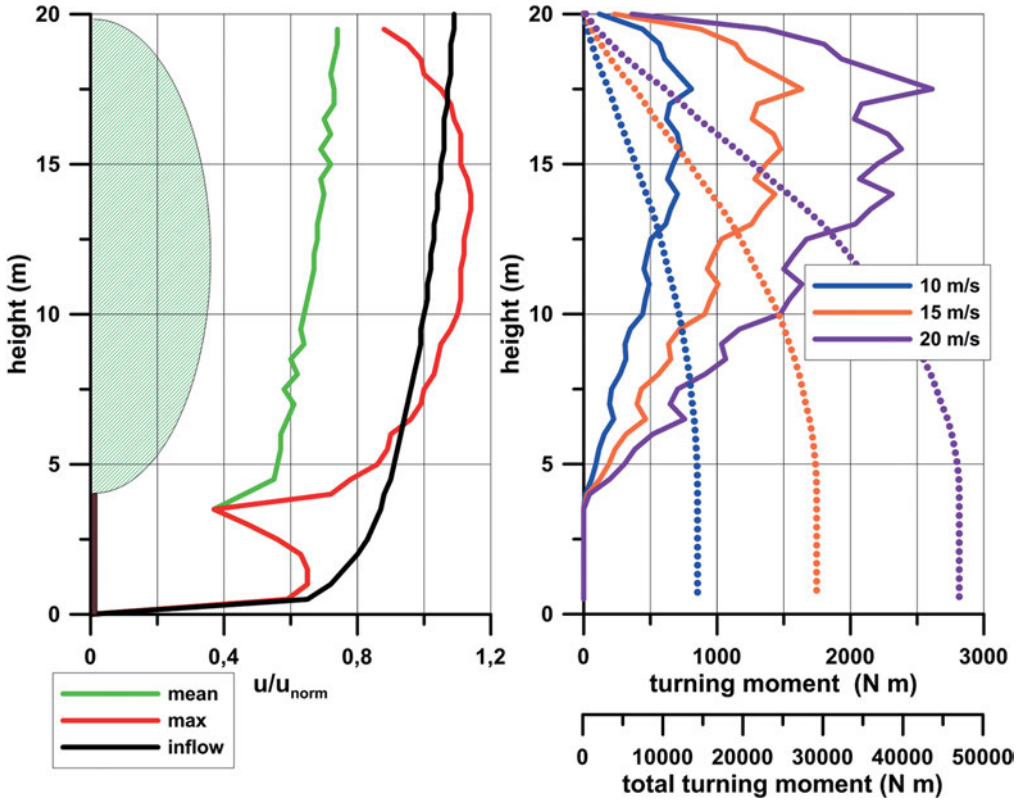

Figure 3: Left: Vertical profiles for mean wind and maximum wind along the windward-side of the tree normalized with the undisturbed 10 m wind. Right: Vertical profiles of local (solid line) and total (dashed line) turning moment for different wind speeds at 10 m.

The mean wind acting on the outer parts of the tree is the important parameter for estimating the load and the risk for windthrow and stem breakage. The simulated near surface distribution around the tree of the local, normalized wind is given in Fig. 2. High wind speeds are calculated in the upper part and in the trunk zone, while the beginning of the wake region is indicated at the lee side.

For calculating the empirical estimates for wind load after e.g. PELTOLA et al. (1999) a representative vertical profile of mean wind is essential. In a first approximation, gusts are included in this calculation by an empirical constant gust factor, but the effects of swaying trees, probably important for specific weather situations, are not considered here. In order to calculate the required vertical distribution, local winds are integrated horizontally along the windward side of the tree. The resulting profile is given in Fig. 3 together with the maximum wind close to the tree surface at different heights and the logarithmic inflow profile. Due to the wind reduction near the obstacle, mean wind around the tree is weaker than the unaffected situation. However, caused by the deflection of the air flow around the tree, maximum wind is slightly larger than the inflow value at the same height.

The force caused by wind action on the crown multiplied by the lever arm results in a turning moment T according to Eq. (2.4). In order to estimate the total turning moment at the base of the stem the contributions of 1-m segments along the stem are calculated and integrated down from tree top to bottom. Such calculations were carried out for different wind speeds, and results are given in Fig. 3. The increasing mean wind speed with height is the reason for the larger values of T in the upper part of the tree, and the stronger the oncoming wind the larger the turning moments for 1-m segments are. The upper part of the tree provides a larger portion to the total turning moment than the lower part with weak winds. For a mean wind at 10 m height between 10 m s^{-1} and 20 m s^{-1}, a maximum turning moment of 15 kN to 45 kN is calculated for the model tree assumed in this study.

However, the results depend strongly on the numerous and specific input data and parameters necessary to calculate the wind force and the resistance of the tree against e.g. uprooting. In a parameter study, the bandwidth of tree load for a variation of different factors is calculated. For the reference run $b = 0.5\,\mathrm{m}^{-2}\,\mathrm{m}^{-3}$, $DBH = 0.21$ m, $G = 2.0$ and $h_{\mathrm{soil}} = 0.7$ m have been chosen as default. The critical wind speeds for uprooting u_{crit}^{UP} and stem breakage u_{crit}^{ST} are used as measures for this comparison. Assuming similarity of the air flow, these values are calculated by successively increasing the wind speed until the thresholds of UP (Eq. (2.6)) and ST (Eq. (2.7)) are attained and exceeded. For the basic parameter set, the simulated critical wind speed for uprooting is $u_{\mathrm{crit}}^{UP} = 17\,\mathrm{m\,s}^{-1}$ and for stem break-

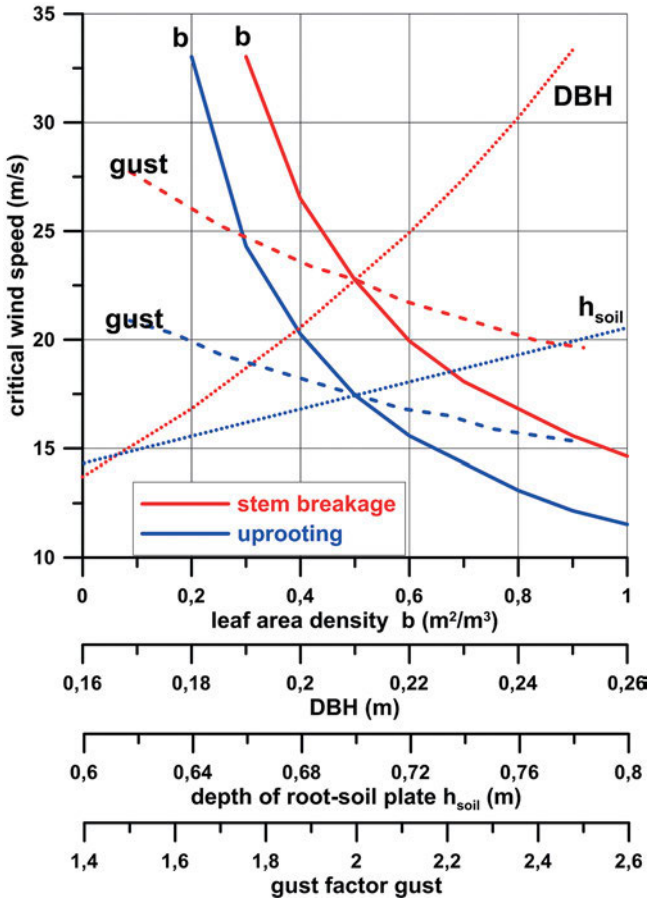

Figure 4: Impact of input data variation on critical wind speed for uprooting and stem breakage.

age is $u_{crit}^{ST} = 23\,m\,s^{-1}$ (Fig. 4). These values are in the order given also in PELTOLA and KELLOMÄKI (1993) where they found corresponding numbers for Scots pine trees with $u_{crit}^{UP} = 10$–$20\,m\,s^{-1}$ and $u_{crit}^{ST} = 20$–$30\,m\,s^{-1}$ depending on taper and crown to stem weight ratio. A strong impact on the critical wind speeds is given by a variation of leaf area density (c_d acts in a similar way) since the acting force on the tree depends directly on this parameter (Eq. (2.1)). For an increase from $b = 0.2\,m^2\,m^{-3}$ up to $1.0\,m^2\,m^{-3}$, critical wind speed for uprooting decreases by a factor of three down to $12\,m\,s^{-1}$. For a variation of the gust factor by ±30 % around the basic value of *gust* = 2.0, u_{crit}^{UP} decreases from $21\,m\,s^{-1}$ to $15\,m\,s^{-1}$ for a higher gustiness of the air flow. One parameter which determines the anchorage of the tree and the resistance against uprooting is the depth of the root-soil plate h_{soil}. For larger values of h_{soil} from 0.6 m to 0.8 m, the root-soil plate becomes heavier and the critical wind speed to uproot the tree increases by about 30 % from $15\,m\,s^{-1}$ to $21\,m\,s^{-1}$. The threshold for stem breakage according to (Eq. (2.7)) is proportional to DBH^3, and therefore critical wind speed u_{crit}^{UP} is increasing drastically for trees with a larger diameter.

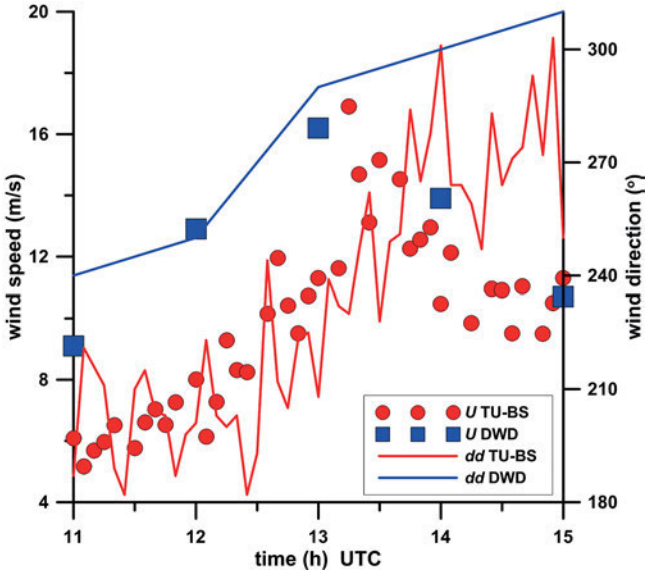

Figure 5: Wind observations on October 5, 2017 at measuring sites of the Technical University of Braunschweig (TU-BS) and of the German Weather Service (DWD).

3.2 Urban tree damage during the storm "Xavier"

Simulated results presented above are encouraging and suggest to use the model system for further studies with regard to wind loads on trees. However, it is important to keep in mind that the robustness and quality of the results depend strongly on the input data and parameters, which are partly unknown or at least inaccurate. Nevertheless, an attempt is made to apply the method to a real storm situation where large damages on urban trees have been observed.

On 5 October 2017, storm "Xavier" passed over the northern part of Germany and caused enormous damage. Train and flight cancellation, power line failures and damage to buildings have been only some of the obvious consequences. With gust wind speeds up to $120\,km\,h^{-1}$ also the larger cities of Hamburg, Hannover and Berlin were hit by the storm. Especially the urban trees were severely affected. For Berlin it is reported that more than 40,000 trees show related damage of various degrees up to a total failure.

Because of the wealth of existing data, a hot spot in the city of Braunschweig was selected as the study area to apply the model system introduced here. Regional mean wind was measured at the rural synoptic station of the German Weather Service DWD and at the university in an urban environment (WEBER, 2017). At the rural site, wind speed increased from $12.9\,m\,s^{-1}$ from 250° at 1200 UTC to a maximum value of $16.2\,m\,s^{-1}$ from 290° at 1300 UTC followed by a sharp decrease (Fig. 5). In general, wind speed at the university measurement station was much lower except for the passage of "Xavier" around 1300 UTC. Also wind direction differed by around 30–40° which might be the result of

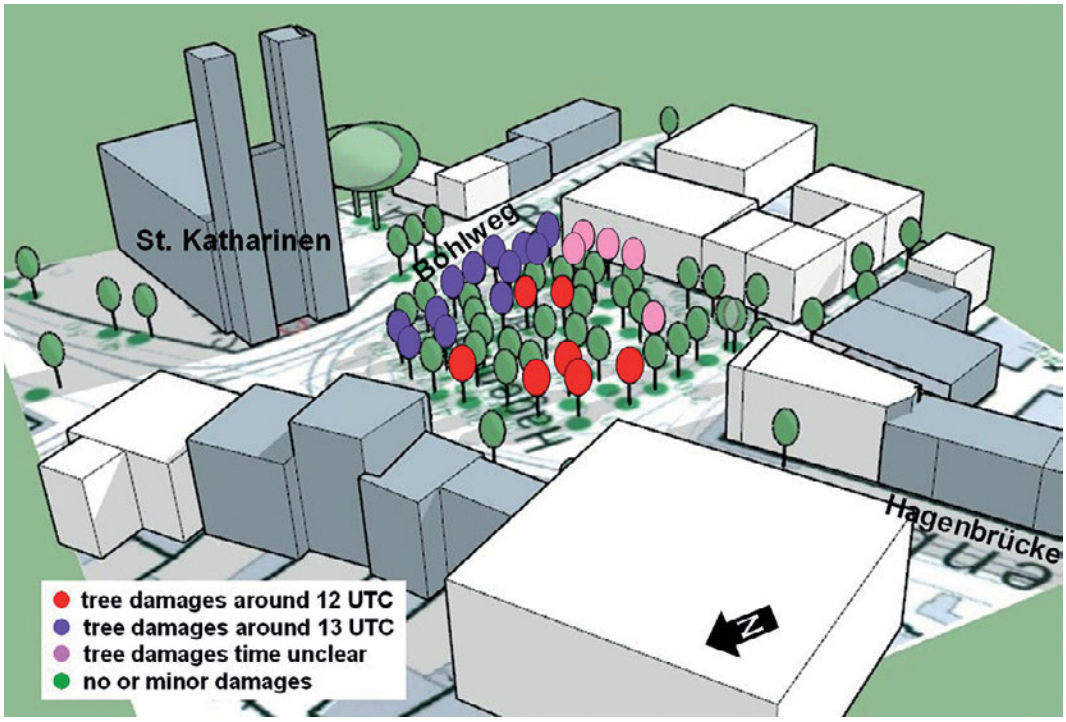

Figure 6: Schematic view of buildings and trees in the simulation region "Hagenmarkt". Coloured trees are damaged during different phases of "Xavier".

the urban environment with a larger number of obstacles and a much higher roughness. However, in general trends in mean wind speed as well as for wind direction were quite similar. Due to the high wind speed, a neutrally stratified atmosphere is assumed here.

Besides the very detailed data for location and height of the individual buildings, also some information about the urban trees according to the tree inventory (BS, 2017) is available. For each tree, species, tree height, *DBH* and diameter of the crown are listed in this database. However, only limited information about anchorage and root system is available. For these and other unknowns, default values described earlier are used. Along roads and sidewalks soil needs to be compacted to withstand traffic loads. In these areas soil for the trees is limited and tree root growth is partly or completely restricted with consequences for the anchorage. Based on a site inspection (Bollmann, 2017) a rough distinction was made for trees growing up within a strong sealing of the soil (e.g. street), a medium sealing (e.g. along sidewalks) and inside the park with sufficient space for the roots. Depending on the location of each individual tree, the anchorage is enhanced for sidewalks ($A_{\mathrm{soil}} = 20\,\%$) and for streets ($A_{\mathrm{soil}} = 10\,\%$).

A schematic view of the local situation around the Hagenmarkt, the hot spot in Braunschweig during storm "Xavier" considered in this study, is given in Fig. 6. The Hagenmarkt is surrounded by multi-storey office and apartment buildings and the church St. Katharinen with a steeple of more than 80 m height. A larger number of urban trees are arranged along the streets and in particular in the park. Nearly all tree species are *Robinia pseudoacacia* of comparable age with a typical height of 15–18 m, a crown diameter of 6–8 m and a diameter at breast height of 0.33–0.38 m. Only south of St. Katharinen two *Platanus acerifolia* have much larger dimensions with a height and a crown diameter larger than 20 m. Buildings and trees are defined on a numerical grid with 1 m grid resolution in all three directions. Above 30 m this grid is expanded up to 4 m at a height of 150 m.

All trees damaged during storm "Xavier" are marked with different colours in this figure. In the first phase of the storm a mean wind from 250° increases continuously up to a strength of 6 on the Beaufort scale (Bf = 6) around 1200 UTC. According to an eyewitness (Riebau, 2017) the first severe wind damage occurred at 1145 UTC and at 1215 UTC when the trees at the northwestern edge of the park as well as at the end of the promenade inside the park facing southeast are windthrown (red trees in Fig. 6). These preferred targets for wind damage have also been reported by videos (BSZ, 2017; Video, 2017). One hour later, in the second phase of the storm, mean wind speeds up to $16\,\mathrm{m\,s^{-1}}$ at 10 m height are observed at the rural station, while wind direction shifts to 290–300°. Now, tree damage up to total failure have been observed along the Bohlweg at the eastern side of the park (Bollmann, 2017) indicated by purple coloured trees in Fig. 6. For trees coloured in pink, observed damage cannot be attributed to any particular time or trees have been removed after the storm for safety reasons.

The location of wind endangered areas with windthrow of trees during the passage of the storm "Xavier"

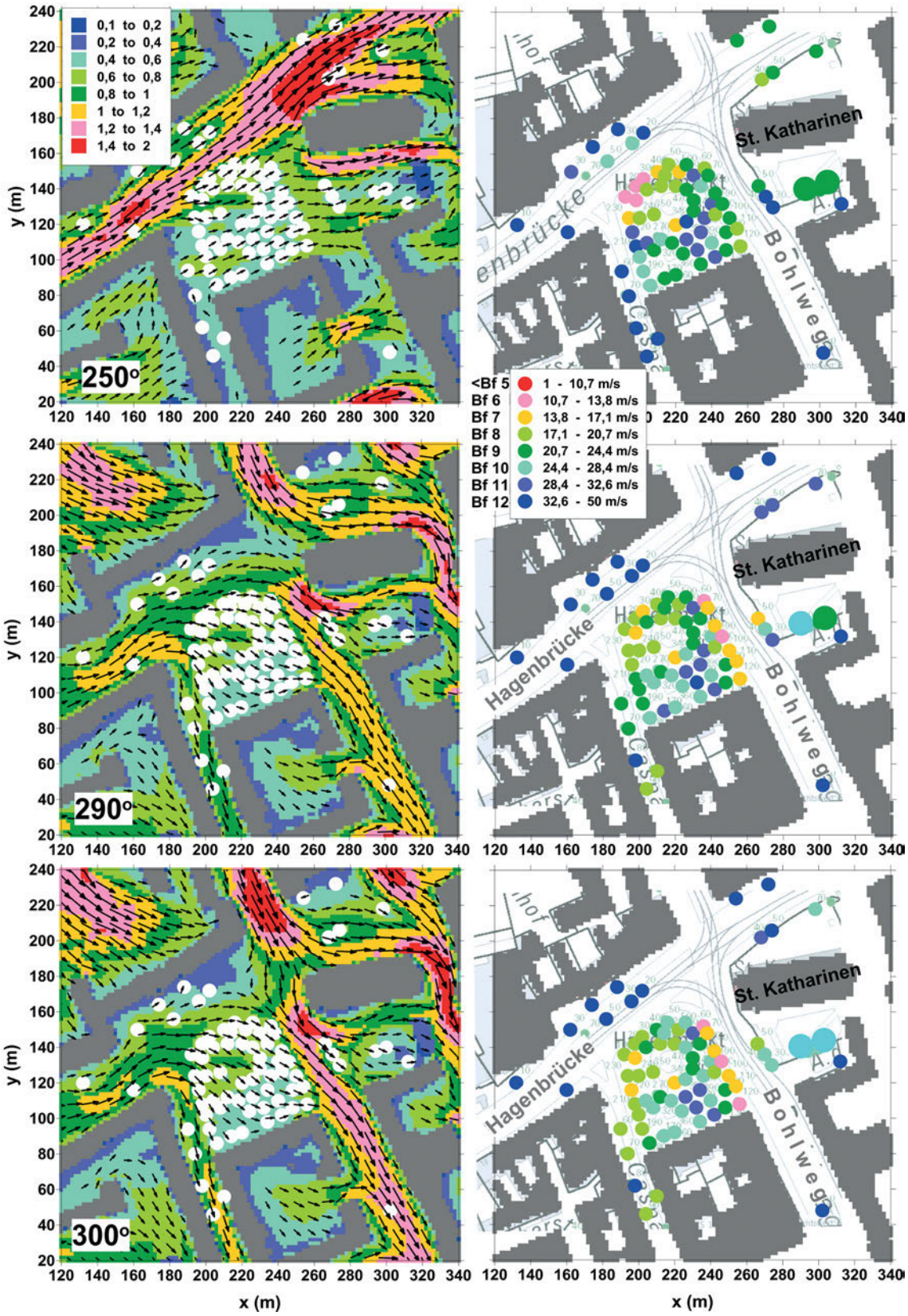

Figure 7: Left: Wind vectors and normalized (reference value is rural 10 m wind) mean wind speed at 10 m above ground for different rural wind directions. Grey blocks: buildings, white circles: trees. Right: Necessary 10 m rural mean wind speed for different wind directions for windthrow of individual trees. Grey blocks: buildings at 2 m height.

are significantly separated and suitable for testing the model system introduced here. For different wind directions *dd* and speeds *U* at the rural DWD-station, the air flow within the complex urban environment has been simulated.

For the 1200 UTC situation with a mean southwesterly wind ($dd = 250°$) of $U = 12.9\,\mathrm{m\,s^{-1}}$ the air flow is channelled within the streets oriented in the same direction while calm situations are simulated else (Fig. 7). Horizontal mean wind at 10 m height is represented in this figure by wind vectors and by wind speed normalized with the value at the rural station. Locally along the streets, mean wind speed is more than 40 % higher than the value of the oncoming wind, increasing the risk for the exposed urban trees significantly. The assessment of the danger level for windthrow is based on the rural wind which must prevail in order to uproot the entire tree. For a rural wind of Bf 6 ($10.7–13.8\,\mathrm{m\,s^{-1}}$) the turning moments exceed root anchorage of the trees at the northwestern corner of the Hagenmarkt. This area is strongly endangered for windthrow at this time. In accordance with observations the numerical model identifies nearly the same location of the most vulnerable urban trees during the first phase of the storm. Also for some other individual trees inside the park an increased risk for winds from Bf 7 on is simulated. The largest wind load is simulated for the trees north of St. Katharinen where a strong increase of the air flow is simulated. However, the anchorage within a sealed and highly compressed near road surface is much larger than in the park with natural soil, and a wind strength of Bf 8 would here be necessary for uprooting at this time.

In the following hour, synoptic wind speed increases up to Bf 7 and wind direction turns to 290–300° (Fig. 7). This change is associated with a complete modification of the urban near surface wind distribution. Now, the calm wind conditions in the north-south running streets are replaced by high wind situations with extreme wind loads on the trees along the Bohlweg. For the complete tree row, a high wind risk for windthrow is simulated for wind strength of 6 to 7 on the Beaufort scale. Again the observations for this time show a large number of uprooted trees in the same area. For this synoptic situation an increased risk for isolated individual trees inside the park is simulated as well. Only uprooting damages are simulated and observed although stem breakage criterion has been calculated as well.

4 Conclusions

A three-dimensional micro-scale model was used to study the interactions of strong winds and individual urban trees. Storms can exert extreme forces resulting in major damage to parts or the entire tree. Besides the physical damage, aesthetic, financial and social losses become a concern to people as well as risk and liability for residents of the surrounding property. These aspects are of special importance for city planners and emergency services.

The model introduced here was used for a parameter study for an individual tree in order to identify important tree parameters for uprooting and stem breakage. In combination with high wind speeds, leaf area density is the most important parameter to estimate the wind force on the tree. A strong anchorage in the soil with a large depth of the root-soil plate prevents uprooting, while larger trunk diameter counteracts very efficiently against stem breakage. This study demonstrates the accuracy of the different input data required for a reliable and promising application of the model. While the above-ground tree information is reasonably available, details in the ground below the tree are sparse with large uncertainties.

During the strong storm event "Xavier" in the northern part of Germany a large number of urban trees were affected and severely damaged. This meteorological situation was used to apply the model for a limited real city environment where detailed information about all individual trees, including the storm damage, has been available. The developed tool was able to identify the nearby areas with observed windthrow of trees for the different phases of the storm.

All numerical experiments show very encouraging results compared to observations and findings from forestry, and applications for real cities can be envisaged as a future prospect and idea. This would allow the identification and mapping of the wind risk of urban trees depending on season (leaf area density) and for different wind speeds and directions. Prior to a storm it would be possible to close probable endangered zones for public safety and to secure buildings for property value. On the other hand, such results could help to optimize future greening and planting to minimize the danger of tree damage to an acceptable level and to guarantee sustainability. In urban areas with a high wind risk estimated by the model, species with limited growth height can be selected, accompanied with appropriate measures for an effective tree anchorage.

It should be mentioned here that the numerical model provides detailed and very valuable insight on wind risk for trees in a complex urban environment. However, shortcomings of this method caused by the lack of input data, model characteristics like grid resolution or parameterizations or effects not included here (e.g. tree sway, soil moisture, pre-damage) define the limits of application.

Acknowledgements

The author would like to thank the reviewer for the extremely valuable comments.

This paper is part of the MOSAIK-project, which is funded by the German Federal Ministry of Education and Research (BMBF) under grant 01LP1601 within the framework of Research for Sustainable Development (FONA; www.fona.de).

References

Bollman, A., 2017: personal communication. – University Hannover.

Bruse, M., 2016: Windrisk und Stadtbäume: Zwischen Stadtklimaverbesserung und Sturmgefahr. – Conference paper FLL Verkehrssicherheitstage 2015, Berlin, https://www.researchgate.net/publication/308415508.

BS, 2017: Baumkataster. – Geoportal FRISBI – Stadt Braunschweig.

BSZ, 2017: braunschweiger-zeitung.de/video

Cermak, J., N. Nadezhdina, M. Trcala, J. Simon, 2015: Open field-applicable instrumental methods for structural and functional assessment of whole trees and stands. – iForest **8**, 226–278.

Coutts, M.P., 1986: Components of tree stability in Sitka Spruce on Peaty Gley soil. – Forestry **59**, 173–197.

Gardiner, B., H. Peltola, S. Kellomäki, 2000: Comparison of two models for predicting the critical wind speeds required to damage coniferous trees. – Ecol. Model. **129**, 1–23.

Gardiner, B., K. Bryrne, S. Hale, K. Kamimura, S.J. Mitchell, H. Peltola, J.-C. Ruel, 2008: A review of mechanistic modelling of wind damage risk to forests. – Forestry **81**, 447–463.

Gromke, C., B. Ruck, 2008: Aerodynamic modelling of trees for small-scale wind tunnel studies. – Forestry **81**, 243–258.

Gross, G., 1993: Numerical simulation of canopy flows. – Springer Verlag Heidelberg.

Gross, G., 2012: Effects of different vegetation on temperature in an urban building environment. Micro-scale numerical experiments. – Meteorol. Z. **21**, 399–412.

Gross, G., 2014: On the estimation of wind comfort in a building environment by micro-scale simulation. – Meteorol. Z. **23**, 51–62.

Gross, G., 2017: Some effects of water bodies on the urban environment – numerical experiments. – J. Heat Island Inst. Inter. **12–2**.

Jäger, S., 2014: Examination of gust wind speed from observations and GFS reanalysis during strong wind events. – Master thesis, KIT Karlsruhe.

Kormas, A., J.M. Prospathopoulos, P.K. Chaviaropoulos, K. Yakinthos, 2016: Wind flow simulation over forested areas using a 3D RANS solver with a tree-scale approach. – J. Wind Eng. Ind. Aerodyn. **155**, 149–158.

Kuttler, W., 2011: Climate change in urban areas, Part 1, Effects. Environmental Science Europe (ESEU). – Springer open, DOI:10.1186/2190-4715-23-11, 1–12.

Lee, H., J. Holst, H. Mayer, 2013: Modification of human-biometeorologically significant radiant flux densities by shading as local method to mitigate heat stress in summer within urban street canyons. – Adv. Meteor **312572**, DOI:10.1155/2013/312572.

Mayer, H., 1985. Baumschwingungen und Sturmgefährdung des Waldes. – Wiss. Mitteilungen **51**, Univ. München, Meteorol. Inst.

Mayer, H., D. Schindler, 2002: Forstmeteorologische Grundlagen zur Auslösung von Sturmschäden im Wald in Zusammenhang mit dem Orkan „Lothar". – Allg. Forst- u. J.-Ztg. **173**, 200–208.

Mayhead, G.J., 1973: Some drag coefficients for British forest trees derived from wind tunnel studies. – Agric. Meteor. **12**, 123–130

Milne, R., 1991: Dynamics of swaying of Picea sitchensis. – Tree Physiology **9**, 383–399.

Mochida, A., Y. Tabata, T. Iwata, H. Yoshino, 2008: Examining tree canopy models for CFD prediction of wind environment at pedestrian level. – J. Wind Eng. Ind. Aerodyn. **96**, 1667–1677.

Peltola, H., S. Kellomäki, 1993: A mechanistic model for calculating windthrow and stem breakage of Scots pines at stand edge. – Silva Fenn. **27**, 99–111.

Peltola, H., S. Kellomäki, H. Väisänen, V.-P. Ikonen, 1999: A mechanistic model for assessing the risk of wind and snow damage to single trees and stands of Scots pine, Norway spruce, and birch. – Can. J. For. Res. **29**, 647–661.

Raupach, M.R., R.H. Shaw, 1982: Averaging procedures for flow within vegetation canopies. – Bound.-Layer Meteor. **22**, 79–90.

Riebau, G., 2017: personal communication. – Braunschweig.

Roloff, A. (Ed.), 2016. Urban Tree Management for Sustainable Development of Green Cities. – John Wiley. Chichester, UK., 274. ISBN 978-1-118-95458-4.

Ruck, B., F. Schmitt, 1986: Das Strömungsfeld der Einzelbaumumströmung. – Forstwiss. Centralbl. **105**, 178–196.

Salim, M.H., K.H. Schlünzen, D. Grawe, 2015: Including trees in the numerical simulations of the wind flow in urban areas: Should we care? – J. Wind Eng. Ind. Aerodyn. **144**, 84–95.

Salmond, J.A., M. Tadaki, S. Vardoulakis, K. Arbuthnott, A. Coutts, M. Demuzere, K.N. Dirks, C. Heaviside, S. Lim, H. Macintyre, R.N. McInnes, B.W. Wheeler, 2016: Health and climate related ecosystem services provided by street trees in the urban environment. – Env. Health **15**, 95–111.

Shashua-Bar, L., M.E. Hoffman, 2004: Quantitative evaluation of passive cooling of the UCL microclimate in hot regions in summer, case study: urban streets and courtyards with trees. Building and Environment 39, 1087–1099.

Video, 2017: https://www.youtube.com/watch?v=0_q-TpFUJ6K.

Weber, S., 2017: personal communication. – University Braunschweig.

Wood, C.J., 1995: Understanding wind forces on trees. – In: Coutts, M.P., Grace, J. (Eds): Wind and wind related damage to trees. – Cambridge University Press, Cambridge, 133–164.